

# An In-Field Calibration Method based on Performance-Surface for the Multiresolution Bilateral Filter Applied to X-Ray Images

Fabiana Fernandes, Cássio Carneiro, Zélia Peixoto and Flávia Freitas

**Abstract**— Several spatial filters applied to images are available in technical and scientific literature. Besides the reduction of the noise level, some of them also aim at the preservation of the edges as well as the details. Those filters are commonly applied to the processing of X-ray medical image sequences, which are usually noised due to the low doses of radiation suitable for medical procedures but where the loss of any detail may impair a diagnosis. In this context, the Bilateral Filter is well suited. Recent papers presented the Multiresolution Bilateral Filter, which embed the Bilateral Filter in the process of Wavelet Denoising. However, the literature lacks a procedure for adjusting the parameters of the Bilateral Filter. Here, we show that an adequate calibration is required for guaranteeing increased performance. We present an in-field calibrating method for Multiresolution Bilateral Filter in order to reduce the noise level and preserve the image edges, built upon the analysis of a Performance-Surface. The proposed method surpasses the performance of the calibration methods that have already been presented in the literature.

**Keywords**— *Multiresolution Bilateral Filter; Image Denoising; X-ray Images; Performance-Surface; Edge Preserving.*

## I. INTRODUCTION

The acquisition of X-ray images is carried out under strict conditions of exposure time of the patient to radiation and X-ray dosage. However, decreasing the dose implies increasing the image noise level suppressing important details and thus hindering the diagnosis. Therefore, denoising of medical X-ray images must be performed assuring the preservation of the characteristics of the image [1].

In those cases, temporal filtering techniques are a good tool for preserving image details, beyond of its low complexity of implementation. However, in sequences of images where some movement is present, e.g. digital angiography for hemodynamic tests, the classic temporal filtering techniques cannot be applied, because they cause trails in the motion direction. Thus, spatial filters may be used instead.

These filters are accomplished with convolution masks applied to the pixels of the image. Usually, they reduce the noise level but they also cause edge smoothing. This shortcoming precludes their use for medical purposes since losses are not commonly allowed in accurate diagnosis. However some spatial filters are more likely to preserve the edges. A suitable example is the bilateral filter, which combines both domain and range filters. The first takes into account the spatial distance between neighboring pixels to calculate the mask weights, while the second is concerned

about the difference between their gray intensities [2]. The calibration of the bilateral filter consists of determining the parameters  $\sigma_d$  (from the domain filter) and  $\sigma_r$  (from the range filter). It is necessary to reach the best cost benefit between reducing the noise level and preserving the image edges, objectives that are conflicting in nature.

Recent papers present the Multiresolution Bilateral Filter (MBF) as a way to improve the capability of reducing noise and preserving image details. The method consists in embedding in the process of wavelet denoising the filtering of the approximation coefficients using the bilateral filter, while the detail coefficients are subjected to some thresholding procedure. The image is reconstructed using IDWT (Inverse Direct Wavelet Transform) and then it is processed by the bilateral filter [3] [4]. In [3] and [5], a procedure for the pursuit of the optimum parameters of the bilateral filter developed for 8-bit images is presented. However, issues related to the calibration of the Multiresolution Bilateral Filter remain for further research and development, as suggested by the authors.

In this paper, we present a calibrating method for the MBF applied to X-ray images, based on the analysis of sensibility of filter performance to the variation of its adjusting parameters, through the inspection of a Performance-Surface. As study cases, angiography images corrupted with different noise levels are filtered in order to show how an optimal calibration can help with performance improving. Comparisons with the MBF using the parameters adjusted according to [3] are also shown.

## II. TECHNICAL BACKGROUND

### A. Bilateral Filter

The bilateral filter was firstly proposed by [2] consisting of a discrete filter applied to the spatial domain, by using a convolution mask, according to the Equation 1,

$$y(k) = \frac{\sum_{n=-N}^N W(n)x(k-n)}{\sum_{n=-N}^N W(n)} \quad (1)$$

where  $W(k)$  weighs the contribution of each neighboring pixel  $x(k-n)$  inside the mask regarding the calculation of the value of the processed pixel  $x(k)$ ,  $k$  is the location of the central pixel of the mask and  $n$  is the distance between the central pixel and its neighbor. The two-dimensional filtering can be performed in two one-dimensional steps.

In the bilateral filter, the contribution  $W(k)$  of each neighboring pixel corresponds to the product of the weight  $W_d(n)$  of a domain filter (that depends on the spatial distance between the two pixels) and on the weight  $W_r(k,n)$  of a range filter (that depends on the difference between the intensities of both) [6]. The weights  $W_d(n)$  and  $W_r(k,n)$  are determined by Equations 2 e 3, in which  $\sigma_d$  and  $\sigma_r$  are adjusting parameters of the decaying curve of the filters weights in function of the spatial distance  $n$  and of the difference of intensities  $x(k-n)$  and  $x(k)$ , respectively. The idea is that if neighboring pixels are very close but significantly different in intensity, they provide a small contribution in the result of the spatial filtering. Thus, the image edges are better preserved and the noise level is reduced mainly in the regions in which intensity levels are more uniform.

$$W_d(n) = \exp\left(-\frac{n^2}{2\sigma_d^2}\right) \quad (2)$$

$$W_r(k,n) = \exp\left(-\frac{(x(k)-x(k-n))^2}{2\sigma_r^2}\right) \quad (3)$$

The calibration of the bilateral filter consists of determining the parameters  $\sigma_d$  and  $\sigma_r$  to achieve the best-cost benefit between reducing the noise level and preserving the image edges.

It was shown in [3] and [5] that the optimum value for  $\sigma_d$  is relatively insensitive to the standard deviation of the noise. However, analyzes accomplished with images corrupted with different noise intensities were performed to investigate the dependence of  $\sigma_r$  regarding the statistical characteristics of the noise. The obtained results led the authors to propose that  $\sigma_r$  can be determined from the product of the standard deviation of the noise by a factor  $R$ , given by  $\sigma_r = R\sigma_{noise}$ . Thus, the calibration is built around finding the optimal  $R$  for a noise with known statistical properties.

### B. Wavelet Denoising

The wavelet denoising process basically follows three steps: decomposition into subbands, thresholding and reconstruction. The first and the third steps consist in the application of the Discrete Wavelet Transform (DWT) and the Inverse Discrete Wavelet Transform (IDWT), respectively, to obtain the approximation and the detail coefficients (Figure 1) and, at the end, the signal reconstruction. To perform these steps, one has to choose the level of multiresolution, which defines how many levels of decomposition the Wavelet Transform will hold as well as the type of wavelet basis to be used. In this paper, the results have been built around wavelet sym8.

The second step, which performs the thresholding of the detail coefficients, is divided into two parts: the calculation of the threshold and then the application of this threshold over the wavelet coefficients [7].

One of the most simple thresholding methods is the UTH: the universal threshold calculated using Equation 4 (in which  $H$  is the number of pixels of the image) is applied to all detail coefficients according to the hard threshold function, which keeps intact the value of the wavelet coefficient if its absolute

value is greater than the calculated threshold. Otherwise, the new value of the coefficient turns to be zero.

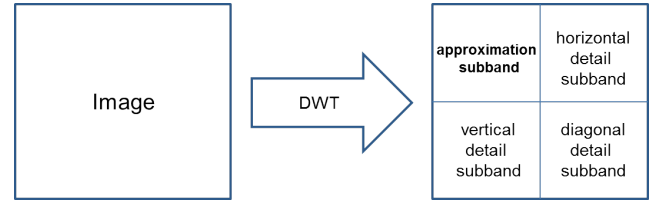


Fig. 1. Wavelet Decomposition

$$\lambda = \lambda_{uni} = \sigma_{noise} \sqrt{2 \log(H)} \quad (4)$$

### C. Multiresolution Bilateral Filter

The idea of the MBF is to embed the bilateral filter in the process of wavelet denoising [3] [4]. This work will present a new procedure for the calibration of two different versions of the Multiresolution Bilateral Filter.

In MBF1 procedure, the image is decomposed using the DWT and then applies the bilateral filter to the approximation coefficients, whereas the detail coefficients are thresholded using the UTH method. Finally, the resulting image is built using the IDWT. MBF2 procedure is identical to the filter MBF1 plus the application of a bilateral filter on the reconstructed image.

The block diagrams of filters MBF1 and MBF2 are shown in Figure 2 (a) and (b), respectively.

In [3] the MBF2 is implemented using  $\sigma_d = 1.8$  e  $\sigma_r = \sigma_{noise}$ , i.e.,  $R=1$ . The same parameters are used for bilateral filter applied to the approximation coefficients and the reconstructed image.

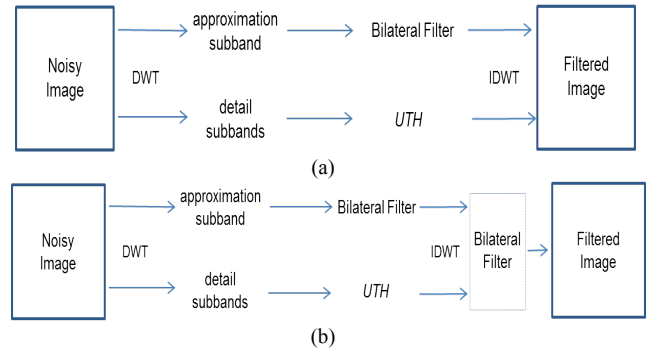


Fig. 2. (a) MBF1 (b) MBF2

## III. THE IN-FIELD CALIBRATION METHOD BASED ON PERFORMANCE-SURFACE

In this article, we present an in-field calibration method for the MBF, based on the sensitivity analysis of the parameters ( $\sigma_d$ ,  $R$ ) of the bilateral filters inserted into the procedures MBF1 and MBF2. The idea is to build a Performance-Surface from the values achieved for a specific metric, collected from experimental results, at several different combinations of ( $\sigma_d$ ,  $R$ ). Thus, the Performance-Surface can provide us a detailed look on how the optimum adjustment parameters can help with the improvement of the MBF's performance, providing the basis for the in-field calibration of

such filters, when they are developed for angiography equipment.

The proposal is dedicated to MBF applied to the filtering of low-doses X-ray images. Thus, in the calibration procedure, an industrial phantom acquired in real conditions of medical procedures is used. The calibration phantom must have density characteristics that simulate different tissues of the human body as well as frequency components that simulate structures presented in the medical procedures, such as blood vessels, bone structures, calcifications and catheters. In this work, also the results of the filtering have been built around the use of phantoms due the difficult of access images of actual exams that have not been digitally processed yet. We consider that the images to be processed are corrupted with Gaussian noise with a specific normalized value of standard deviation, here named  $\sigma_{noise}$ .

Beyond the PSNR (Peak Signal to Noise Ratio), which is a metric that is commonly used in digital image processing, we chose another metric for the determination of the Performance-Surface: MSSIM (Mean Measure Structural Similarity) [8]. The MSSIM has the intention of providing a good perception of the HVS (Human Vision System). While PSNR is measured in dB, MSSIM varies in the range of 0 to 1 and evaluates quantitatively how close the output image is to the reference image, in terms of intensity, structure and contrast. Best results are reflected in values of MSSIM near to value 1.

In order to calibrate the bilateral filter applied to the approximation coefficients, both implemented in MBF1 and MBF2, the following procedure is performed: after the decomposition of the calibration phantom image by DWT, the bilateral filter is applied to the approximation coefficients using several pre-established pairs of values for the parameters  $(\sigma_d, R)$  whereas the UTH method is applied to the detail coefficients. The resultant image, considering each pair  $(\sigma_d, R)$ , is built using the IDWT and the selected metric is calculated. The values of the metric associated to each pair  $(\sigma_d, R)$  are used to plot a Performance-Surface over the plane  $(\sigma_d, R)$ . The regions of the plane  $(\sigma_d, R)$  corresponding to the best performances are then identified and used to calibrate the bilateral filter. With this procedure, the calibration of the bilateral filter of the MBF1 is complete.

However, for the MBF2, it is still necessary to calibrate the bilateral filter applied to the reconstructed image. This is accomplished as follows: the parameters of the bilateral filter used in the approximation coefficients, already calibrated, are held constant whereas the detail coefficients are submitted to UTH method and the resultant image is reconstructed by IDWT. Finally, the sensitivity analysis of the bilateral filter applied to the resultant image takes place for the same pairs of parameter values  $(\sigma_d, R)$ , used in the last step. The obtained values for the selected metric are used to yield the Performance-Surface, which describes the filter performance according with the parameters  $(\sigma_d, R)$ . In the same way as described, the regions of the plane  $(\sigma_d, R)$  that allow for improvement of the performance are identified and used to calibrate this bilateral filter.

## IV. IMPLEMENTATION

### A. Image Used in the Calibration

During the calibration procedure, the phantom image must be processed by the MBF and the filtered image is then compared to a reference image in order to compute the metrics. Since a reference image is not available during the experiments, it is obtained from a temporal average calculated over 8 frames of the calibration phantom, acquired at different times. The calibration phantom is shown in Figure 3.

The value of  $\sigma_{noise}$  is estimated from the histogram of the difference between one of the noisy image frames and the reference image after normalizing their pixels. The calibration phantom image was acquired with the equipment AngiX III FD, manufactured by Brazilian company Xpro. The normalized estimated value for  $\sigma_{noise}$  was 0.026.

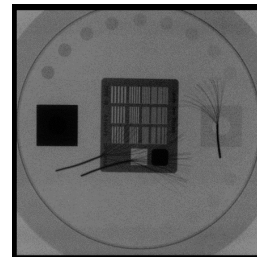


Fig. 3. Calibration phantom

### B. The Calibration

The performance and the sensitivity analyses of the bilateral filters applied to the approximation coefficients (embedded in MBF1 and MBF2) were accomplished by varying  $\sigma_d$  from 0.5 to 5, in steps of 0.5, and by varying  $R$  from 0.5 to 10, in steps of 0.5. The metrics PSNR and MSSIM were calculated for the calibrating phantom image for each  $(\sigma_d, R)$  pair.

Figures 4 and 5 provide the visualization of PSNR and MSSIM gains. The gains refer to the difference between the metrics for the filtered image and the metrics for the noisy image. It can be noticed that the best performance of the bilateral filter is achieved for values of  $\sigma_d$  larger than or equal to 2.5, approximately. The lower the value of  $\sigma_d$ , the larger the expected value of  $R$  aiming at optimizing performance.

The calibration of the bilateral filter applied to the reconstructed image, which is only embedded in MBF2, was then performed. Both parameters  $\sigma_d$  and  $R$  were varied in the same ranges and steps previously described. Similarly, the metrics PSNR and MSSIM were calculated using each aforementioned pair of values  $(\sigma_d, R)$  to yield the corresponding Performance-Surfaces. Figures 6 and 7 provide visualization of PSNR and MSSIM gains.

It is interesting to observe that PSNR is more sensitive to variations of the adjusting parameters than MSSIM, which was not expected. It is also worth mentioning that, in the regions corresponding to the pairs  $(\sigma_d, R)$  that provide the largest performance of the filter (i.e, regions where  $\sigma_d$  and  $R$  assume very small values), variations of PSNR and MSSIM gains are virtually unnoticeable.

## V. RESULTS AND DISCUSSION

From the calibration process described in the previous section,  $\sigma_d=3$  was chosen for the calibration of all the bilateral filters (the one applied to approximation coefficients as well as the one which operates on the reconstructed image) using either PSNR or MSSIM. The values of  $R$ , in turn, were determined from the normalized graphs corresponding to the chosen metrics, PSNR or MSSIM, considering that  $\sigma_d=3$ . Table 1 summarizes the chosen values of  $R$  using PSNR or MSSIM during the calibration.

After the calibration procedure, MBF1 and MBF2 were used to reduce the noise level (while preserving edges) at images of a test phantom, also acquired by AngiX III FD, in equivalent conditions of real medical procedures.

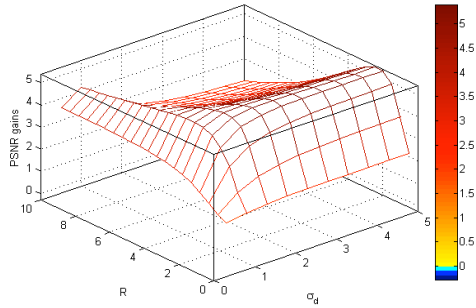


Fig. 4. PSNR gains (dB) as a function of  $\sigma_d$  and  $R$  (bilateral filter applied to the approximation coefficients)

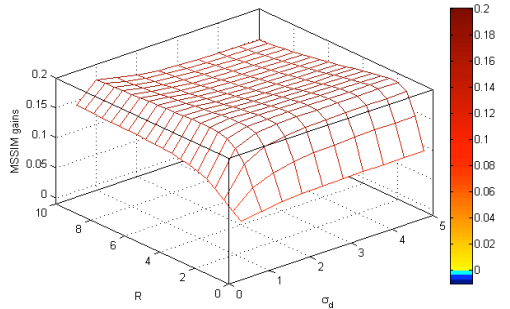


Fig. 5. MSSIM gains as a function of  $\sigma_d$  and  $R$  (bilateral filter applied to the approximation coefficients)

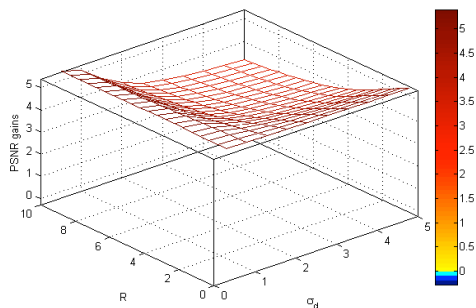


Fig. 6. PSNR gains (dB) as a function of  $\sigma_d$  and  $R$  (bilateral filter applied to the reconstructed image)

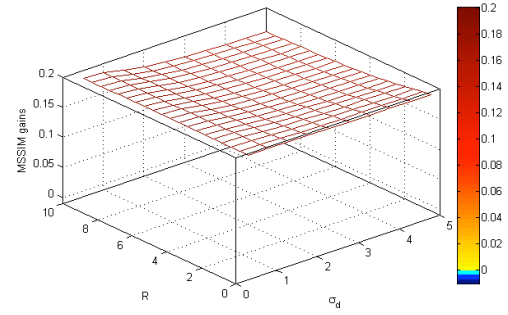


Fig. 7. MSSIM gains as a function of  $\sigma_d$  and  $R$  (bilateral filter applied to the reconstructed image)

Figures 10, 11 and 12 show the images after filtering. The correspondent noisy image and the reference image are depicted at Figures 8 and 9, respectively. It can be verified from a subjective analysis that the MBF2 [3] (Fig.10) does not reduce the noise level as expected. On the other hand, the MBF2 (Fig.12) calibrated accordingly to our proposal, that is, with basis on the Performance-Surface, presents some losses at the edges. Thus, the MBF1 calibrated using the Performance-Surface outperforms the others and is elected as the best filtering option, since it achieves the best cost-benefit between reducing the noise and preserving the edges.

TABLE I - CHOSEN VALUES FOR  $R$  FROM USING EITHER PSNR OR MSSIM DURING CALIBRATION.

Filter being calibrated	PSNR	MSSIM
Bilateral Filter applied to approximation coefficients (both MBF1 and MBF2)	2.5	2.5
Bilateral Filter applied to reconstructed image (MBF2)	0.5	0.5

TABLE II - PSNR AND MSSIM GAINS USING AN IMAGE FROM THE TEST PHANTOM.

Multiresolution Bilateral Filter	PSNR gains	MSSIM gains
MBF2 [3]	2.35	0.09
MBF1 (PSC by using PSNR or MSSIM)	3.08	0.1
MBF2 (PSC by using PSNR or MSSIM)	2.86	0.09

## VI. CONCLUSIONS

Recent papers present the Multiresolution Bilateral Filter as a way to improve the capability of reducing noise and preserving image details. However, the literature lacks a clear and efficient procedure to calibrate the parameters of this filter. Fortunately, from calibration procedures presented in [3] and [5] for the bilateral filter we were able to present a new and accurate in-field calibration procedure to find the values of the parameters of the filter that optimize either PSNR or MSSIM using an X-ray phantom image. The denoising process of X-ray images using the Multiresolution Bilateral Filter properly calibrated gave us a superior result in terms of noise level reduction and edge preservation, when comparing to works presented in recent literature. This was verified not only from metrics calculated from phantom images but also from visual

inspection. Moreover, it is worthwhile to mention that the in-filed Performance-Surface Calibration procedure can be accomplished with any other metrics that can be found in order to better approximate the HSV perception. In this context, the specialist can also apply his own subjective evaluation to determine the pair of parameter values that optimizes the image quality of the phantom and then use these parameters to calibrate the filters that will be applied during the actual medical procedures.

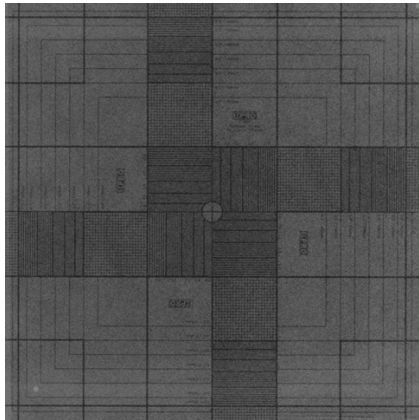


Fig. 8. Noisy Image

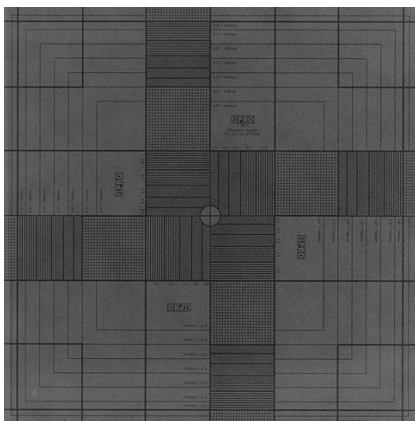


Fig. 9. Reference Image

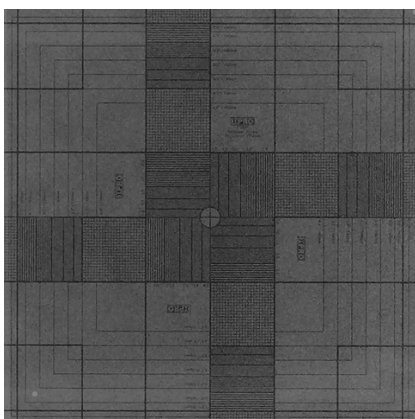


Fig. 10. MBF2 [3]

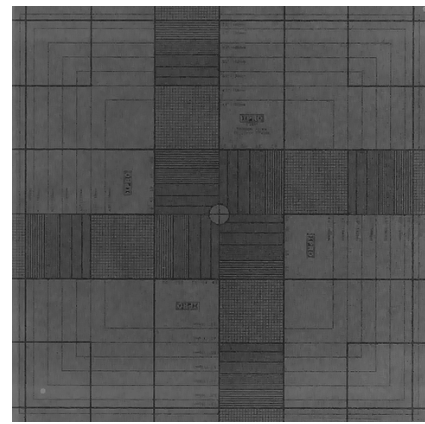


Fig. 11. MBF1 (SPC by using PSNR or MSSIM)

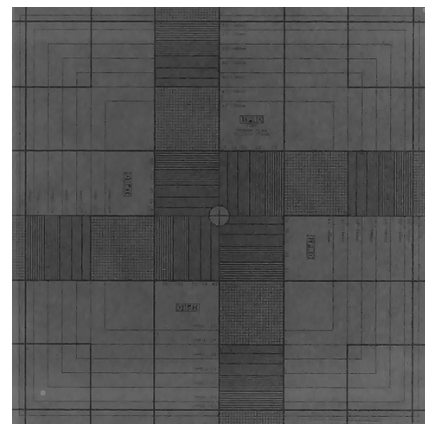


Fig. 12. MBF2 (SPC by using PSNR or MSSIM)

## REFERENCES

- [1] L. Zhang, J. Chen, Y. Zhu and Z. Luo, "Comparisons of Several New De-Noising Methods for Medical Images," in *3rd International Conference on Bioinformatics and Biomedical Engineering*, Beijing, 2009.
- [2] C. Tomasi and R. Manduchi, "Bilateral Filtering for Gray and Color Images," in *IEEE International Conference on Computer Vision*, Bombay, 1998.
- [3] M. Zhang e B. K. Gunturk, "Multiresolution Bilateral Filtering," *IEEE Transactions on Image Processing*, vol. 17, n. 12, December 2008.
- [4] V. Vanithamani and G. Umamaheswari, "Wavelet based Despeckling of Medical Ultrasound Images with Bilateral Filter," in *IEEE Region 10 Conference - TENCN*, Bali, 2011.
- [5] A. Gabiger-Rose, M. Kube, P. Schmitt, R. Weigel and R. Rose, "Image Denoising Using Bilateral Filter With Noise-Adaptive Parameter Tuning," in *37th Annual Conference on IEEE Industrial Electronics Society*, Melbourne, 2011.
- [6] J. Giraldo, Z. Kelm, L. Guimaraes, L. Yu, J. Fletcher, B. Erickson and C. McCollough, "Comparative Study of Two Image Space Noise Reduction Methods for Computed Tomography: Bilateral Filter and Nonlocal Means," in *31st Annual International Conference of the IEEE EMBS*, Minneapolis, Minnesota, USA, 2009.
- [7] K. Fodor and C. Kamath, "On Denoising Images Using Wavelet-Based Statistical Techniques," 1996.
- [8] Z. Wang, A. Bovik, H. Sheikh and E. Simoncelli, "Image Quality Assessment: From Error Visibility to Structural Similarity," *IEEE Transactions on Image Processing*, vol. 13, pp. 600-612, April 2004